IEEE Access
Multidisciplinary | Rapid Review | Open Access Journal

Received September 26, 2018, accepted October 10, 2018, date of publication October 23, 2018,
date of current version November 19, 2018.

Digital Object Identifier 10.1109/ACCESS.2018.2877637

A Frequency-Reconfigurable Tuner-Loaded Coupled-Fed Frame-Antenna for All-Metal-Shell Handsets

CHONG-ZHI HAN[1], GUAN-LONG HUANG[1], (Member, IEEE), TAO YUAN[1], WONBIN HONG[2], (Senior Member, IEEE), AND CHOW-YEN-DESMOND SIM[3], (Senior Member, IEEE)

[1]ATR National Key Laboratory of Defense Technology, College of Information Engineering, Shenzhen University, Shenzhen 518060, China
[2]Department of Electrical Engineering, Pohang University of Science and Technology, Pohang 37673, South Korea
[3]Department of Electrical Engineering, Feng Chia University, Taichung 40724, Taiwan

Corresponding author: Guan-Long Huang (guanlong.huang@szu.edu.cn)

This work was supported in part by the National Natural Science Foundation of China under Grants 61701320 and 61801300, in part by the Shenzhen Science and Technology under Grant JCYJ20170818101347761, in part by the State Key Laboratory of Millimeter Waves under Grant K201932, and in part by the New Teacher Natural Science Research Project of Shenzhen University under Grant 2018078.

ABSTRACT A frequency-reconfigurable frame-antenna integrated with a coupling strip and tuner loading is proposed for all-metal-shell mobile telephones. The coupling strip introduces additional capacitance to the feeding structure of the antenna, rendering the antenna to resonate at both the lower frequency band at ''a quarter-wavelength resonant mode'' and the higher frequency band at ''a half-wavelength resonant mode''. Moreover, the antenna loaded with a tuner achieves broadband frequency-reconfiguration by tuning the effective length of radiating frame. The antenna is designed by taking into consideration all the metallic components, like front-and-back cameras, telephone receiver, and a steel sheet. The metal-frame and metal-shell of the handset coupled with a strip are used as parts of the antenna. This paper of a prototype operating in a practical handset test environment shows that the proposed antenna is able to cover the bandwidth of 824–960 MHz (GSM) and 1710–2690 MHz (DCS/PCS/UMTS/LTE) with acceptable radiation efficiency up to 40% and desirable patterns and specific absorption ratio, which is much lower than 1.6 W/kg for mobile communications.

INDEX TERMS Frequency-reconfigurable, all-metal-shell handset, coupling strip, tuner, frame-antenna.

I. INTRODUCTION

Antenna for all-metal-shell handset devices have been one of the most critical design challenges in recent years, especially when the handset has possessed very limited metal clearance, because most of the available spaces are occupied by radio-frequency (RF) components such as front-and-back-facing cameras, full-display screen, battery, and so forth. The metal clearance is normally referred to the space between the antenna and its nearest metallic structure/component in the handset, which is necessary for the antenna to radiate signal. Therefore, the space available for placing the antennas is always limited to a very small volume size, thus results in withholding the handset antenna's design freedom.

Several handset/tablet antenna designs have been reported for metal-shell (metal-casing) applications [1]–[4]. Amid these designs, [1] has reported the used of two separate open-end slots to achieve dual-band characteristic for covering the LTE/WWAN bands (690-960 MHz and 1700-2700 MHz). To achieve multiple resonances with two broadband operations for the LTE/WWAN bands, a metal-frame antenna with two Inverted-F antennas (IFAs) was investigated in [2]. Here, in order to generate desirable radiations for the LTE/WWAN operations, three asymmetric open-slots have also been applied into the two IFAs, which are supported by a high-pass and band-pass matching circuits [2]. Nevertheless, the work reported in [3] for a half-loop metal-frame antenna has also applied two different matching circuits (low- and high-pass) to cover the LTE/WWAN bands, in which it further requires an elevated feed network (with four grounding strips) to link to the open-slot on the metal-frame.

Recently, antenna designs for metal-frame smart-phones have made significant progress [4]–[7]. Similar to the works in [1]–[3], by utilizing the metal-frame as part of the antenna,

the dual-loop antennas reported in [4] and [5] are capable to cover GSM/DCS/PCS/UMTS/LTE2300/2500 operating bands. Other kinds of antenna designed for smart-phone have also been discussed in [8]–[15], in which [9] has reported a reconfigurable loop antenna that uses RF switch to cover a wider bandwidth by adjusting the four working states of the switch, while the other works in [10]–[15] have adopted the monopole antenna design type. Even though some of these metal-frame designs have yielded good bandwidth characteristic for smart-phone applications, they have also occupied large metallic areas that are used as the metal-shell of the handset [16]–[18]. Furthermore, in order to gain enough metal clearance, a large space has to be subtracted from the metal-shell, which significantly decrease the appearance and the robustness of the handset. Therefore, an all-metal-shell (not just metal-frame) handset is presently considered for future mobile handset devices. Nevertheless, due to the growing challenges in all-metal-shell handset antennas in terms of multiple band operations and tunable frequency range, it is necessary to introduce the frequency reconfiguration technologies (via the pin diodes, switches or varactors) to widen the operational bands [16]–[18], in which a tuner might be a good candidate for all-metal-shell handset antenna, because of its continuous adjustability, better parasitic parameter and flexible application scenarios [18].

In this paper, a frequency-reconfigurable frame-antenna with a coupling strip and a RF tuner for all-metal-shell handset application is proposed to cover the 824-960 MHz (GSM) and 1710-2690 MHz (DCS/PCS/UMTS/LTE) operating bands. The continuously adjustable tuner used in this case is able to offer more desirable working states compared with conventional RF switch. Compared with other antenna designs for smartphone application that have also covered the two aforementioned operating bands [19]–[24], this proposed work has considered a practical handset environment. It is also noteworthy that within a practical handset, because of the existence of the front-and-back cameras, telephone receiver and other RF components which occupy most of the spaces available in the handset limited volume spaces for the metal clearance is inevitable, thus significantly increasing the difficulty of the antenna design. Because such practical design environment is rarely mentioned in other research works therefore, the main objective of this work is to propose a practical approach to develop a frequency-reconfigurable frame-antenna in an all-metal-shell handset environment with desirable performances while maintaining its appearance.

II. ANTENNA DESIGN IN HANDSET ENVIRONMENT

Fig. 1 shows the environment of an all-metal-shell handset model where the proposed antenna is installed. In this figure, different layers of the handset together with a zoomed view of the coupling strip and feed point are also included. In order to demonstrate the main structures clearly, dielectric materials have been hidden. The antenna is configured using the metal-frame as the main radiator while the metal-shell acts as the antenna ground. Two cameras, a telephone receiver and other

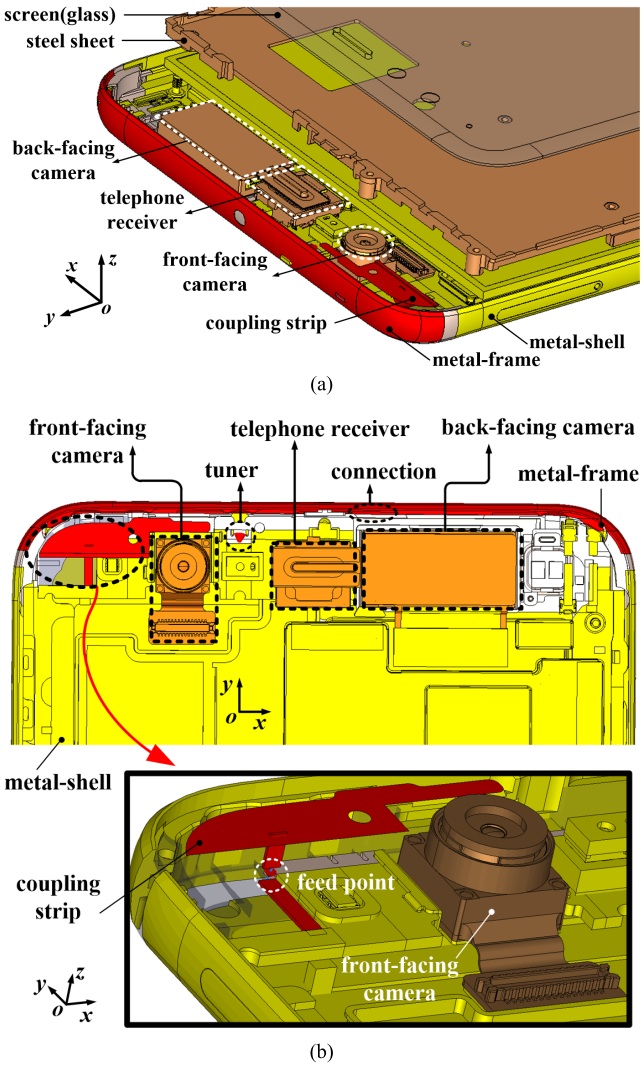

FIGURE 1. Configuration of the antenna in the handset environment (a) Explosive-view of the handset. (b) Zoomed view of the proposed antenna in the handset environment.

metallic structures/components which occupy the finite space of the handset have been taken into consideration during the antenna design process.

During the simulation design process, the handset model as shown in Fig. 1(a) is mainly composed of four sections indicated by four colors as follows: (1) the transparent gray color refers to the handset screen (glass: $\varepsilon_r = 4.82$) on top; (2) the yellow color refers to the metal-shell (copper) of the handset; (3) the brown color indicates perfect electric conductor (PEC), which is applied to the antenna's peripheral components such as the steel sheet, dual-back-facing camera, front-facing camera and the telephone receiver; (4) the red color is referring to the coupling strip that is laser-engraved on the Acrylonitrile Butadiene Styrene (ABS: $\varepsilon_r = 2.4$) substrate via the Laser Direct Structuring (LDS) technology. Here, the coupling strip and the metal-frame are also copper but they are changed to red color so as to make

them more recognizable. Fig. 1(b) shows the zoomed view of the proposed antenna, which includes the metal-frame as the radiator, the coupling strip as the feeding structure, and the metal-shell as the antenna ground.

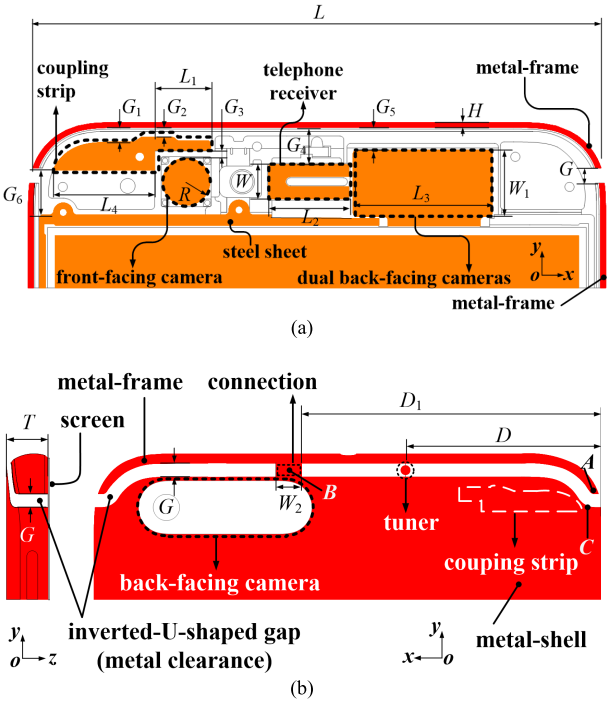

FIGURE 2. Geometry of the proposed antenna in the handset environment with peripheral metal components. (a) Top-view. (b) Bottom-view.

The detailed geometry of Fig. 1 is illustrated in Fig. 2. In this figure, the telephone receiver is placed close to the middle of the metal-frame with size $L_2 \times W$, the front-facing camera has a radius R, and the back-facing camera is with dimension $L_3 \times W_1$. As it is obvious that all of these metallic components will limit the metal clearance space and because of that, electromagnetic wave can be easily reflected/absorbed among these components, thus, the distance between the antenna body and the nearby metallic components will definitely affect the radiation performance. The other parameters shown in Fig. 2 are illustrated as follows: the gap between the coupling strip and the front-facing camera is G_3, while G_4 and G_5 indicate the distance of the metal-shell away from the telephone receiver and the dual-back-facing camera, respectively. The spacing between the coupling strip and the steel sheet is G_5, the thickness of the handset is T and that of the metal-frame is H. Here, a 2-mm symmetric inverted-U-shaped gap is used to separate the metal-frame and the metal-shell, which act as the metal clearance for the proposed antenna.

As shown in Fig. 2(a), the antenna radiator (metal-frame) is fed by a coupling strip of length L_1+L_4, and the function of this coupling strip is to introduce additional capacitance to the feeding structure, enabling the antenna to excite two resonant modes, namely, the 0.25λ and a 0.5λ mode that can cover the lower (824-960 MHz) and higher (1710-2690 MHz) operating bands, respectively (λ stands for the effective wavelength with surrounding environment). To understand the excitation of these two resonant modes, one can observe Fig. 2(b), in which the current distributions of these two modes will be excited in point A (metal-frame) and flowing towards point C (metal-shell) via a ground connector at point B. Hence, this current distribution route $A - B - C$ can be considered as a customized loop antenna. Here, the connector should be wide enough (W_2) to achieve a better separation between the loop antenna and the top-left corner of the handset, as the latter, in general will be used to place another antenna for the Global Positioning System (GPS) application. Furthermore, the location of the connection (point B), represented by D_1, will affect the resonant bands of the loop antenna as it is relevant to the length of the loop. Nevertheless, the coupling-feed method applied in this work is superior to a traditional loop antenna with direct-feed as it can compensate a large inductive reactance introduced by the 0.25λ resonant mode.

During the design process in the handset environment, as shown in Fig. 2(a), it is noteworthy that the distance G_6 (between the coupling strip and the steel sheet) is found to be a crucial parameter relevant to antenna efficiency. Even though the typical gap distance between the coupling strip and the metal-frame of the handset is G_1, due to the irregular-shape of the coupling strip, at certain places, this gap is narrowed down to G_2 Notably, G_1 and G_2 are the two relevant parameters that will affect the input impedance (by introducing additional capacitance) at the feed point. Lastly, to realize frequency-reconfigurable characteristic for the two resonant modes, a tuner is allocated at a distance D away from the opening section of the loop, as shown in Fig. 2(b). All the key parameters in this design are tabulated and presented in Table 1. Detailed effects of the coupling strip on antenna performance will be studied in the following sections. Essential discussion on the tuner and the radiation principle will also be elaborated. The experimental results of the proposed antenna are also included and discussed to verify the feasibility of the scheme.

TABLE 1. Optimized geometric parameters for the proposed antenna.

Parameter	Value (mm)	Parameter	Value (mm)
G	2.0	L	74.2
G_1	1.5	L_1	7.3
G_2	0.9	L_2	10.6
G_3	0.8	L_3	18.3
G_4	4.5	L_4	13.2
G_5	2.6	W	4.2
G_6	4.0	W_1	8.5
H	0.8	W_2	2
D	30.8	D_1	41.8
T	5		

III. OPERATING MECHANISM

To better understand the operating mechanism of the proposed frame-antenna in the all-metal-shell handset,

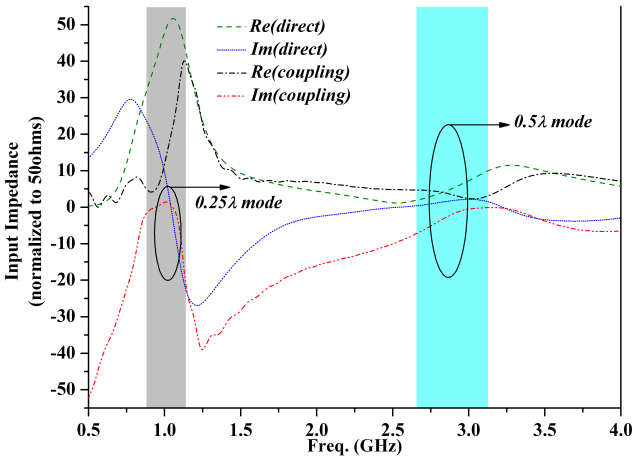

FIGURE 3. Comparison of the simulated real and imaginary parts of the input impedance for the coupling-feed and the direct-feed.

the antenna is firstly investigated as a conventional loop antenna with direct-feed, and a comparison with the coupling-feed proposed in this work is also conducted. Fig. 3 shows the normalized input impedance (to 50 ohms) of the direct-feed loop antenna type, and due to the limited length of the handset, it can only excite a 0.5λ resonant mode at higher frequency band, because the imaginary part of the direct-feed type is very large at lower frequency band According to the resonance theory, once the antenna is expected to resonate at the lower frequency band as 0.25λ resonant mode, it is necessary to introduce a capacitive reactance to compensate the inductance at the feed point. To alleviate this problem, the coupling-feed designed in this work is able to offer an additional capacitance to offset the inductance, in which the matching effect can be controlled by tuning parameters G_1 and G_2.

By fine tuning the parameters via the full-wave electromagnetic software CST Microwave Studio®, two desired resonant modes can hereby be excited by introducing the coupling-feed technique. A comparison of the input impedance of the two cases (coupling-feed and direct-feed) can also be observed in Fig. 3. The lower band is produced by the first resonant mode (0.25λ resonant mode) at around 1000 MHz, and the higher band is formed by the second resonant mode (0.5λ resonant mode) at around 2900 MHz. To further illustrate the excitation of these two resonant modes, the surface current distributions at both the lower and higher bands are plotted in Fig. 4. As presented in Fig. 4(a), a quarter-wavelength loop mode at 1000 MHz can be observed along the metal-frame via the route from point X to point Z. As shown in Fig. 4(b), the second resonant mode has demonstrated a 0.5λ resonant mode, because there are two current null points between the two maximum points (points X and Z), indicating the surface currents reverse phase at point T. The two sub-figures in Figs. 4(a) and (b) have denoted the curves of surface current plotted.

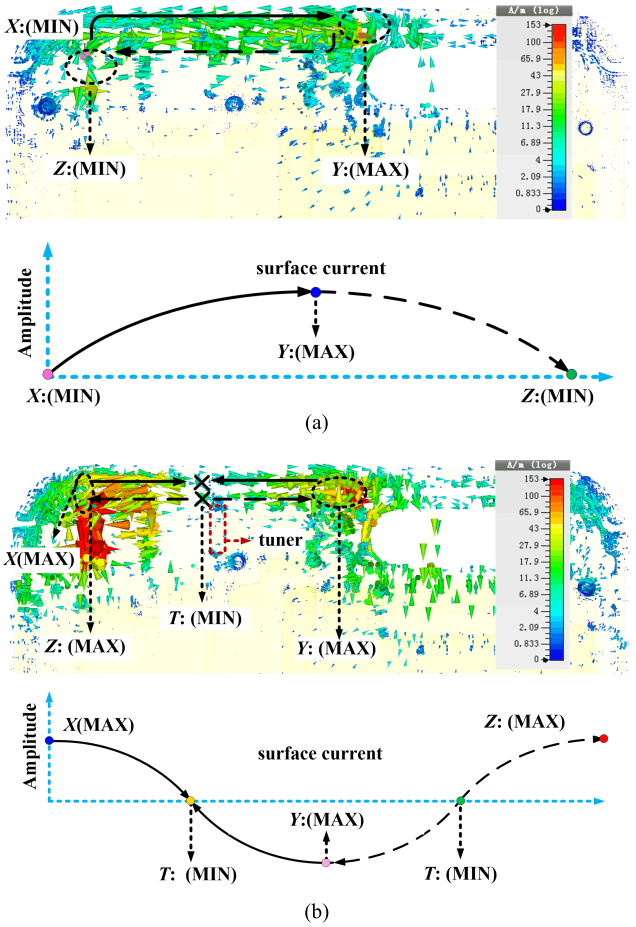

FIGURE 4. Surface current distribution of the proposed antenna at "0.25λ and 0.5λ resonant modes" (a) Surface current distribution at lower band of "0.25λ resonant mode" (1000 MHz). (b) Surface current distribution at higher band of "0.5λ resonant mode" (2900 MHz).

As the operating bandwidths of these two resonances at this stage are not wide enough to cover the desired operating bands (824-960 MHz) and (1710-2690 MHz) for GSM, DCS, PCS, UMTS and LTE applications, therefore, a tuner is introduced, which is essentially a variable capacitor, which can widen the operating bandwidths. The tuner adopted here is a high-voltage-tolerant, highly precise and low-loss tunable capacitor ideal for tunable antennas application. After applying the tuner, it can be observed from Fig. 5 that the two resonances can be shifted to lower frequency band with a larger capacitor-loading. When the tuner is adjusted from 0.75 pF to 3.1 pF, the two resonances are able to cover the two desired bands. Other than the tuning range of the tuner, further investigation from the simulation has also found that the location of the tuner can also affects the range of the frequency tuning. Here, the best location for placing the tuner is the current null point at the surface current distribution, as shown in Fig. 4(b), which is also the point where the electric-field is at its maximum strength. Notably, this optimized location is also marked in Fig. 2(b), which is associated with parameter D.

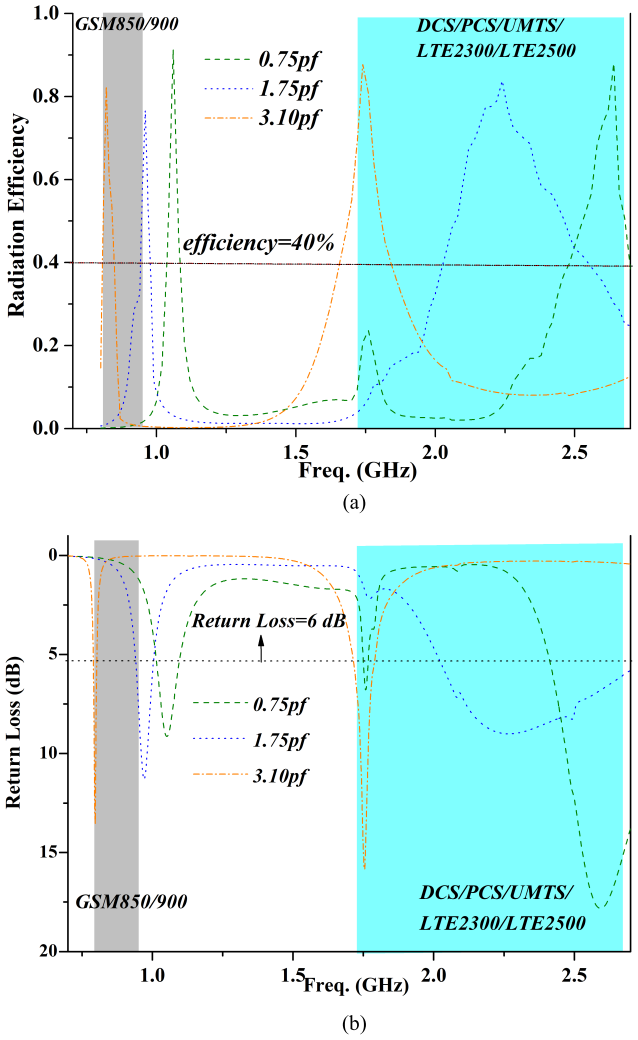

FIGURE 5. Simulated return loss and efficiency of the proposed antenna with different capacitor-loading. (a) Simulated efficiency. (b) Simulated return loss.

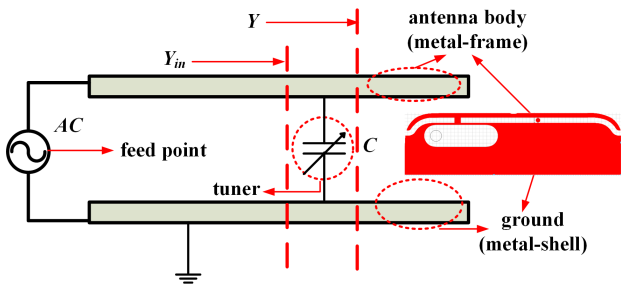

FIGURE 6. Equivalent model of the antenna loaded with the tuner.

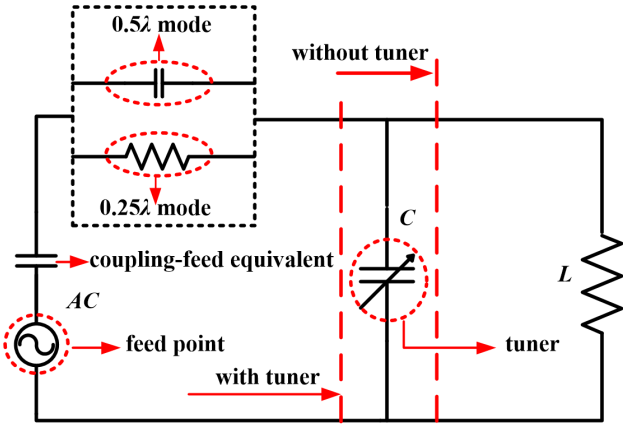

FIGURE 7. Equivalent circuit model of the antenna to illustrate the effect of the tuner-loading.

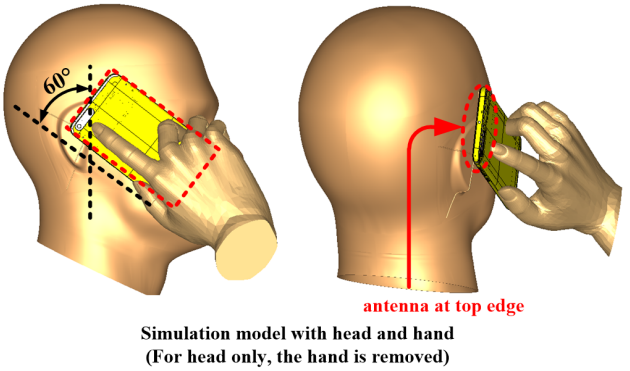

FIGURE 8. SAR simulation model for head only and head & hand tissues.

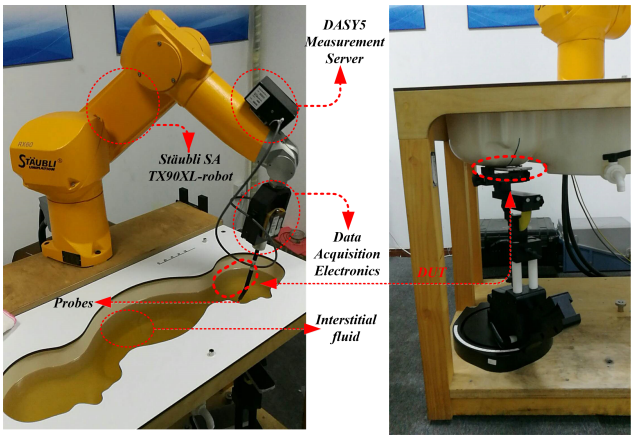

FIGURE 9. Measured SAR simulation model for head only and head & hand tissues.

Fig. 6 demonstrates the equivalent model of the frame-antenna loaded with the tuner. Assuming that the input admittance without the tuner is represented by Y, while that with the tuner is Y_{in} (looking from the feed point to the tuner). The relationship between Y_{in} and Y is denoted in (1), where C stands for the equivalent capacitance of the tuner. The ratio of $K = Y_{in}/Y$ is used to evaluate the effect of the tuner. According to (2), a smaller Y causes a more significant influence on the input admittance of the proposed antenna. In order to increase the sensitivity of the capacitive tuner to the input admittance, the tuner has to be located at the place where Y reaches its minimum value. From this point of view, an appropriate location of the tuner is possible to be located

TABLE 2. Simulated and measured SAR of 1-G head only and head & hand tissues.

Frequency (MHz)	Head only (W/kg)	Head & Hand (W/kg)
900	1.075(simulated)	1.306(simulated)
	1.100(measured)	1.423(measured)
1900	0.707(simulated)	0.893(simulated)
	0.972(measured)	1.217(measured)
2400	0.401(simulated)	0.445(simulated)
	0.583(measured)	0.599(measured)

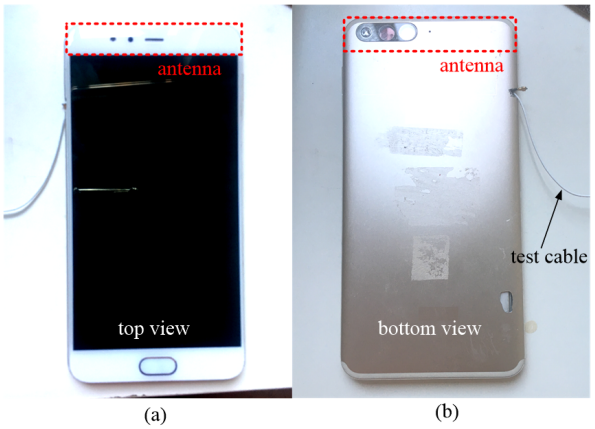

FIGURE 10. Antenna prototype in the handset environment (hidden in the handset body).

FIGURE 11. Antenna under test in the SATIMO measurement system

via theoretical analysis and simulation as aforementioned.

$$Y_{in} = Y + j\omega C \tag{1}$$

$$K = \frac{Y_{in}}{Y} = 1 + \frac{j\omega C}{Y} \tag{2}$$

An equivalent circuit model of the frame-antenna is demonstrated in Fig. 7, so as to evaluate the effects of the shunt capacitive tuner. In analogy with microstrip line, the portion of the frame-antenna between the feed point and the tuner are equivalent to a series-inductor at 0.25λ resonant mode and more likely a series-capacitor at 0.5λ resonant mode, corresponding to the current distributions presented in Fig. 4. In this case, (3)-(5) are established to evaluate the influence of the tuner. When calculating the equivalent inductance L' by taking the effect of the tuner into account, one can get $L' > L$ (L is the equivalent inductance without the tuner), indicating the equivalent length of the

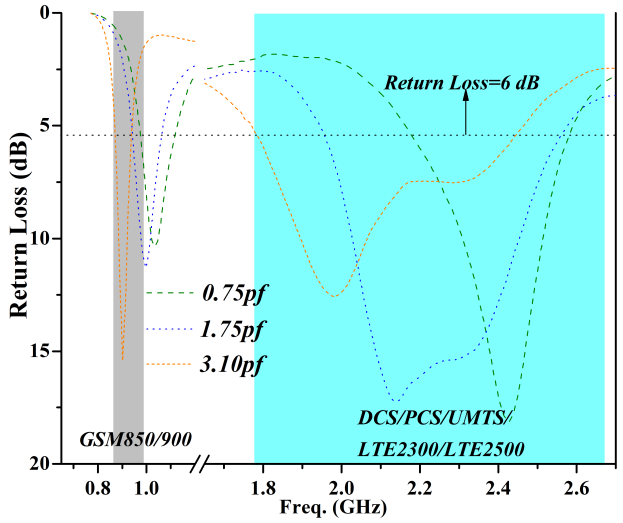

FIGURE 12. Measured return loss of the proposed antenna with different values of capacitor-loading.

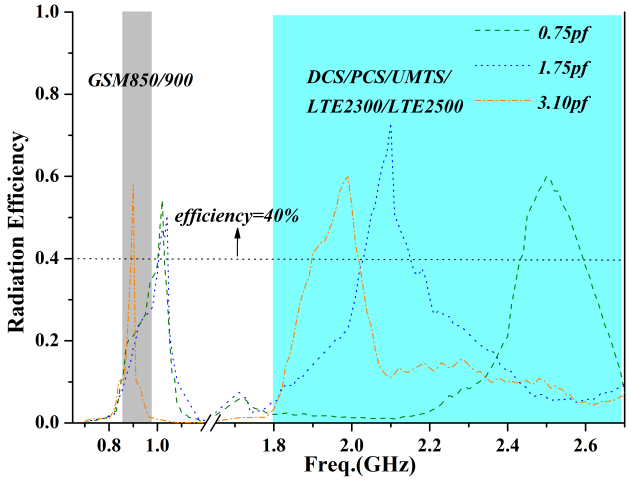

FIGURE 13. Measured efficiency of the proposed antenna with different values of capacitor-loading.

loaded frame-antenna is longer than the one without loading. According to the microstrip line theory, a larger inductance value means a longer electrical length. Therefore, it can be concluded that loading the tuner (which works as a shunt capacitor) can effectively enlarge the equivalent length of the frame-antenna, which in turn will allow the resonances to be tuned to a lower frequency band for both the 0.25λ and 0.5λ resonant modes.

$$Y = \frac{1}{j\omega L} \tag{3}$$

$$Y_{in} = \frac{1}{j\omega L} + j\omega C = \frac{1}{j\omega}\frac{1-\omega^2 LC}{L} \tag{4}$$

$$L' = \frac{L}{1-\omega^2 LC} \tag{5}$$

Figs. 8 and 9 shows the head & hand model of the proposed antenna under simulation and measured environment. The simulated and measured specific absorption rate (SAR) for 1-gram head only and head & hand tissues for typical fre-

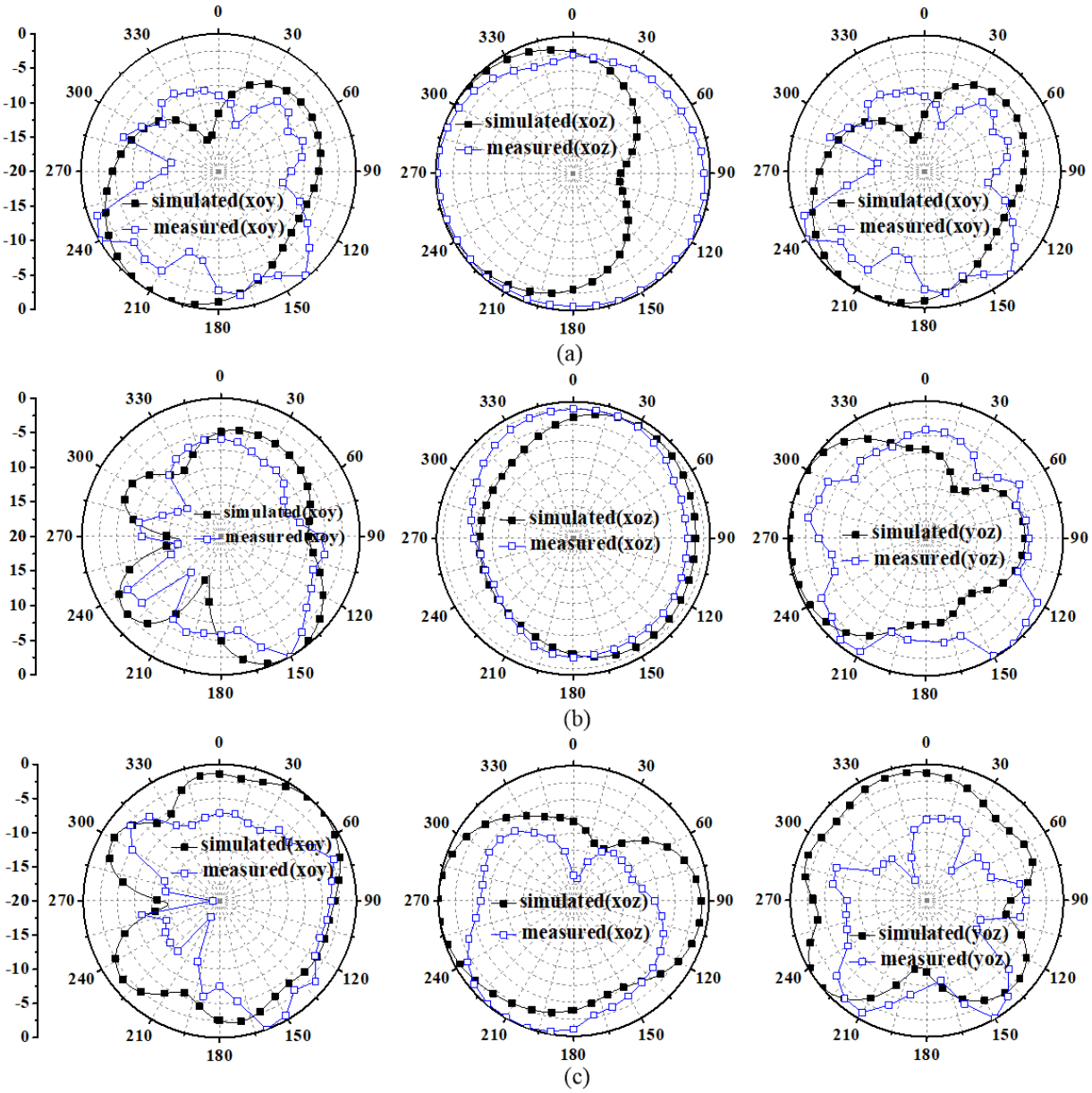

FIGURE 14. Simulated and measured radiation patterns of the proposed antenna at three typical frequencies: (a) 900 MHz; (b) 1900 MHz; (c) 2400 MHz in xoy-, xoz- and yoz-plane (linear polarization).

quencies (at 900 MHz, 1900 MHz and 2400 MHz) are listed in Table 2 The simulated and the measured results show that they are much lower than 1.6 W/kg, which is regulated by the Federal Communications Commission (FCC).

IV. EXPERIMENTAL RESULTS

To verify the frequency-reconfigurable performance of the proposed antenna, a prototype has been fabricated and tested in the handset environment. The coupling strip was built on an ABS substrate with permittivity $\varepsilon_r = 3.3$. The final antenna prototype that is integrated into a practical handset model can be viewed in Fig. 10. Here, a 50 Ω mini coaxial cable is used as the test cable during the measurement. Fig. 11 shows the handset antenna test environment in a SATIMO anechoic chamber.

The measured return losses and efficiencies of the prototype antenna are shown in Figs. 12 and 13, respectively. By tuning the tuner between 0.75 pF and 3.10 pF, frequency-reconfigurable performance can be attained within the 824-960 MHz band (for Bands 1, 2, 5 and 8) and 1710-2690 MHz band (for UMTS, DCS, PCS and LTE bands) with return loss $>$ 6 dB. Furthermore, the radiation efficiencies measured across the two desired bands have varied between 40% and 70%. According to practical engineering requirement and application, satisfactory user experience can be obtained as long as the antenna has an efficiency of more than 30%.

The simulated and the measured radiation patterns of the antenna operating within the lower and higher bands at 900 MHz, 1900 MHz and 2400 MHz are illustrated in Fig. 14.

TABLE 3. Performance comparison among different works.

References	Occupied Space	Operating Bandwidth	Peak Efficiency	Take peripheral metallic components into account?
[7]	55×5×3 mm^3	136 MHz (low-band)	60% (low-band)	no
		980 MHz (high-band)	80% (high-band)	
[9]	75×7×13 mm^3	262 MHz (low-band)	65% (low-band)	no
		980 MHz (high-band)	80% (high-band)	
[19]	70×10×5 mm^3	262 MHz (low-band)	60% (low-band)	only USB
		980 MHz (high-band)	70% (high-band)	
[25]	70×5×7 mm^3	136 MHz (low-band)	60% (low-band)	no
		980 MHz (high-band)	70% (high-band)	
Proposed	41.8×5×2 mm^3	290 MHz (low-band)	60% (low-band)	yes
		980 MHz(high-band)	70% (high-band)	

Here, the simulated and measured data coincides well with each other. Table 3 presents a comparison between the proposed frame-antenna and other published designs. The comprehensive comparison shows that the proposed antenna in this work has occupied lesser space with satisfactory performance, not to mention that the work has considered a practical handset environment in which all the peripheral metallic components are taken into account. Therefore, this investigation has verified that the proposed antenna design is feasible for all-metal-shell handset application.

V. CONCLUSION

A frequency-reconfigurable frame-antenna with coupling-feed has been developed for all-metal-shell handsets. A tuner was introduced to achieve frequency reconfigurable design. With full consideration of the practical handset environment surrounding by metallic electronic components, desirable dual-band bandwidths, stable radiation patterns, and high efficiency of up to 40% are achieved across the 824-960 MHz and 1710-2690 MHz operating bands, which cover the required GSM/ DCS/ PCS/ UMTS/ LTE bands for mobile communications.

REFERENCES

[1] C.-K. Chang, W.-J. Liao, and C.-C. Tsai, "Metal body-integrated open-end slot-antenna designs for handset LTE uses," *IEEE Trans. Antennas Propag.*, vol. 64, no. 12, pp. 5436–5440, Dec. 2016.

[2] K.-L. Wong and C.-Y. Tsai, "IFA-based metal-frame antenna without ground clearance for the LTE/WWAN operation in the metal-casing tablet computer," *IEEE Trans. Antennas Propag.*, vol. 64, no. 1, pp. 53–60, Jan. 2016.

[3] K.-L. Wong and C.-Y. Tsai, "Half-loop frame antenna for the LTE metal-casing tablet device," *IEEE Trans. Antennas Propag.*, vol. 65, no. 1, pp. 71–81, Jan. 2017.

[4] Y. L. Ban, Y. F. Qiang, Z. Chen, K. Kang, and J. H. Guo, "A dual-loop antenna design for hepta-band WWAN/LTE metal-rimmed smartphone applications," *IEEE Trans. Antennas Propag.*, vol. 63, no. 1, pp. 48–58, Jan. 2015.

[5] H.-B. Zhang, Y.-L. Ban, Y.-F. Qiang, J. Guo, and Z.-F. Yu, "Reconfigurable loop antenna with two parasitic grounded strips for WWAN/LTE unbroken-metal-rimmed smartphones," *IEEE Access*, vol. 5, pp. 4853–4858, 2017.

[6] K.-L. Wong and Y.-C. Chen, "Small-size hybrid loop/open-slot antenna for the LTE smartphone," *IEEE Trans. Antennas Propag.*, vol. 63, no. 12, pp. 5837–5841, Dec. 2015.

[7] J.-W. Lian, Y.-L. Ban, Y.-L. Yang, L.-W. Zhang, C.-Y.-D. Sim, and K. Kang, "Hybrid multi-mode narrow-frame antenna for WWAN/LTE metal-rimmed smartphone applications," *IEEE Access*, vol. 4, pp. 3991–3998, 2016.

[8] H. Wang *et al.*, "Small-size reconfigurable loop antenna for mobile phone applications," *IEEE Access*, vol. 4, pp. 5179–5186, 2016.

[9] H.-D. Chen, H.-W. Yang, and C.-Y.-D. Sim, "Single open-slot antenna for LTE/WWAN smartphone application," *IEEE Trans. Antennas Propag.*, vol. 65, no. 8, pp. 4278–4282, Aug. 2017.

[10] C.-Z. Hani, G.-L. Huang, Z.-P. Zhong, T. Yuan, and M.-L. Fan, "A loop antenna with coupling strip and tuner for all-metal-shell handset application," in *Proc. Cross Strait Quad-Regional Radio Sci. Wireless Technol. Conf.*, Xuzhou, China, Jul. 2018, pp. 1–3.

[11] Y.-L. Ban, Y.-F. Qiang, Z. Chen, K. Kang, and J. L.-W. Li, "Low-profile narrow-frame antenna for seven-band WWAN/LTE smartphone applications," *IEEE Antennas Wireless Propag. Lett.*, vol. 13, pp. 463–466, 2014.

[12] Y.-L. Ban, C.-L. Liu, Z. Chen, J. L.-W. Li, and K. Kang, "Small-size multiresonant octaband antenna for LTE/WWAN smartphone applications," *IEEE Antennas Wireless Propag. Lett.*, vol. 13, pp. 619–622, 2014.

[13] Y.-L. Ban, C. Li, C.-Y.-D. Sim, G. Wu, and K.-L. Wong, "4G/5G multiple antennas for future multi-mode smartphone applications," *IEEE Access*, vol. 4, pp. 2981–2988, 2016.

[14] Y.-L. Ban, S. Yang, Z. Chen, K. Kang, and J. L.-W. Li, "Decoupled planar WWAN antennas with T-shaped protruded ground for smartphone applications," *IEEE Antennas Wireless Propag. Lett.*, vol. 13, pp. 483–486, 2014.

[15] M.-Y. Li *et al.*, "Eight-port orthogonally dual-polarized antenna array for 5G smartphone applications," *IEEE Trans. Antennas Propag.*, vol. 64, no. 9, pp. 3820–3830, Sep. 2016.

[16] Y.-L. Ban, Z. X. Chen, Z. Chen, K. Kang, and J. L.-W. Li, "Reconfigurable narrow-frame antenna for heptaband WWAN/LTE smartphone applications," *IEEE Antennas Wireless Propag. Lett.*, vol. 13, pp. 1365–1368, 2014.

[17] Z.-Q. Xu, Y.-T. Sun, Q.-Q. Zhou, Y.-L. Ban, Y.-X. Li, and S. S. Ang, "Reconfigurable MIMO antenna for integrated-metal-rimmed smartphone applications," *IEEE Access*, vol. 5, pp. 21223–21228, 2017.

[18] M. Stanley, Y. Huang, H. Wang, H. Zhou, Z. Tian, and Q. Xu, "A novel reconfigurable metal rim integrated open slot antenna for octa-band smartphone applications," *IEEE Trans. Antennas Propag.*, vol. 65, no. 7, pp. 3352–3363, Jul. 2017.

[19] K.-C. Lin, C.-H. Lin, and Y.-C. Lin, "Simple printed multiband antenna with novel parasitic-element design for multistandard mobile phone applications," *IEEE Trans. Antennas Propag.*, vol. 61, no. 1, pp. 488–491, Jan. 2013.

[20] Y. Yang, Z. Zhao, W. Yang, Z. Nie, and Q.-H. Liu, "Compact multimode monopole antenna for metal-rimmed mobile phones," *IEEE Trans. Antennas Propag.*, vol. 65, no. 5, pp. 2297–2304, May 2017.

[21] Y.-J. Chou, G.-S. Lin, J.-F. Chen, L.-S. Chen, and M.-P. Houng, "Design of GSM/LTE multiband application for mobile phone antennas," *Electron. Lett.*, vol. 51, no. 17, pp. 1304–1306, Aug. 2015.

[22] S.-C. Chen, C.-C. Huang, and W.-S. Cai, "Integration of a low-profile, long-term evolution/wireless wide area network monopole antenna into the metal frame of tablet computers," *IEEE Trans. Antennas Propag.*, vol. 65, no. 7, pp. 3726–3731, Jul. 2017.
[23] F.-H. Chu and K.-L. Wong, "Internal coupled-fed dual-loop antenna integrated with a USB connector for WWAN/LTE mobile handset," *IEEE Trans. Antennas Propag.*, vol. 59, no. 11, pp. 4215–4221, Nov. 2011.
[24] H. Chen and A. Zhao, "LTE antenna design for mobile phone with metal frame," *IEEE Antennas Wireless Propag. Lett.*, vol. 15, pp. 1462–1465, 2016.
[25] Y.-L. Ban, Y.-F. Qiang, G. Wu, H. Wang, and K.-L. Wong, "Reconfigurable narrow-frame antenna for LTE/WWAN metal-rimmed smartphone applications," *IET Microw. Antennas Propag.*, vol. 10, no. 10, pp. 1092–1100, Apr. 2016.

CHONG-ZHI HAN received the B.E. and M.E. degrees in electronic information engineering from the Harbin Institute of Technology, Harbin, China. He is currently pursuing the Ph.D. degree in information and communication engineering with Shenzhen University, Shenzhen, China. His current research interests include the development and application of MIMO antennas and millimetre wave antenna.

GUAN-LONG HUANG (M'11) received the B.E. degree in electronic information engineering from the Harbin Institute of Technology, Harbin, China, and the Ph.D. degree in electrical and computer engineering with the National University of Singapore, Singapore. He serves as the Deputy Director for the Guangdong Provincial Mobile Terminal Microwave and Millimeter-Wave Antenna Engineering Research Center. Prior to join the university, he has been with Temasek Laboratories, National University of Singapore, as a Research Scientist, and the Nokia Solutions and Networks System Technology as a Senior Antenna Specialist from 2011 to 2017. He is currently an Assistant Professor with the ATR National Key Laboratory of Defense Technology, College of Information Engineering, Shenzhen University, Shenzhen, Guangdong, China. His research interests include planar antenna array design and implementation, 5G base-station and mobile RF front-end devices, phased antenna array, channel coding for massive MIMO application, and 3-D printing technology in microwave applications. He is currently serving as an Associate Editor for the IEEE Access.

TAO YUAN received the bachelor's and master's degrees from Xidian University, China, and the Ph.D. degree from the National University of Singapore, Singapore. He is currently a Professor with the College of Information Engineering, Shenzhen University, Shenzhen, China. His current research interests include developing novel RF modules and antennas for mobile terminal and 5G applications.

WONBIN HONG (S'04–M'09–SM'14) received the B.S. degree in electrical engineering from Purdue University, West Lafayette, IN, USA, in 2004, and the master's and Ph.D. degrees in electrical engineering from the University of Michigan, Ann Arbor, MI, USA, in 2005 and 2009, respectively. From 2009 to 2016, he was with Samsung Electronics, Suwon, South Korea, as a Principal and Senior Engineer participating and leading extensive research and development tasks for upcoming wireless applications, including MIMO, wireless power transfer, and millimeterwave wireless solutions. He is currently with the Department of Electrical Engineering, Pohang University of Science and Technology, Pohang, South Korea, as an Assistant Professor. His patented invention on optically invisible microwave antennas for Wi-Fi and GPS in 2016 and has led to over three million commercialized productions as of 2017. He has authored and co-authored over 50 peer-reviewed journals, conference papers, and two book chapters, and is an inventor of over 60 patent inventions. He has over a decade of extensive research and development experience with primary interest in future wireless communication antennas and RF circuits, mesoscale and nanoscale transparent electronics, and 3-D packaging. He is a member of the Technical Committee of IEEE MTT-6 Microwave and Millimeter-Wave Integrated Circuits. He was a recipient of numerous recognition, including the Outstanding Researcher of the Year Award, the Outstanding Mentor of the Year Award, the Major Achievement Award, the Annual Inventor Award, and the Samsung Best Paper Award during his tenure at Samsung. He was also awarded several fellowships and scholarships, including the Samsung Scholarship Award for Graduate Studies, the Rappaport Wireless Scholarship, the NASA Summer Undergraduate Research Fellowship, the A.F. Welch Scholarship, and the Donald McQuinn Scholarship. He is currently serving as an Associate Editor for the IEEE Transactions on Antennas and Propagation and a Guest Editor of the IEEE Transactions on Antennas and Propagation Special Edition on Antennas and Propagation Aspects of 5G Communications. He has served as an invited lecturer and speaker in over 50 international research symposiums, government, and industry sessions held around the world.

CHOW-YEN-DESMOND SIM (M'07–SM'13) was born in Singapore in 1971. He received the B.Sc. degree from the Engineering Department, University of Leicester, U.K., in 1998, and the Ph.D. degree from the Radio System Group, Engineering Department, University of Leicester, in 2003. From 2003 to 2007, he was an Assistant Professor with the Department of Computer and Communication Engineering, Chienkuo Technology University, Changhua, Taiwan. In 2007, he joined the Department of Electrical Engineering, Feng Chia University (FCU), Taichung, Taiwan, as an Associate Professor, where he became a Full Professor in 2012 and a Distinguish Professor in 2017. He is currently serving as the Executive Officer for the Master's Program with the College of Information and Electrical Engineering (Industrial Research and Development), the Director of Intelligent IoT Industrial Ph.D. Program, and the Director of the Antennas and Microwave Circuits Innovation Research Center, FCU. He has authored or co-authored over 110 SCI papers. His current research interests include antenna design, VHF/UHF tropospheric propagation, and RFID applications. He is a fellow of the Institute of Engineering and Technology, a Senior Member of the IEEE Antennas and Propagation Society, and a Life Member of the IAET. He served as the TPC member for the APMC 2012, APCAP 2015, IMWSBio 2015, CSQRWC 2016, ICCEM 2017, APCAP 2018, and CIAP 2018. He was a recipient of the IEEE Antennas and Propagation Society Top 10 Outstanding Reviewer Award for Year (2013–2014), (2014–2015), (2015–2016), and (2016–2017). He has also served as the TPC Sub-Committee Chair (Antenna) for the ISAP 2014 and PIERS 2017. He is currently serving as the Advisory Committee for the InCAP2018. He has served as the TPC Chair for the APCAP 2016 and the Chapter Chair of the IEEE AP-Society, Taipei Chapter, from 2016 to 2017. He has been the Founding Chapter Chair of the IEEE Council of RFID, Taipei Chapter, since 2017. He is currently serving as the Associate Editor for the IEEE AWPL, the IEEE Access,and the *International Journal of RF and Microwave Computer-Aided Engineering* (Wiley). Since 2016, he has been serving as the Technical Consultant of the Securitag Assembly Group, which is one of the largest RFID tag manufacturers in Taiwan. He was invited as the Workshop Speaker at the APEMC 2015 and iAIM 2017, and an Invited Speaker of the TDAT 2015, iWAT 2018, and APCAP 2018. He is the Keynote Speaker of SOLI 2018.